



**HAL**  
open science

## Surface polaritons of a left-handed curved slab

Mounir Faddaoui, Antoine Folacci, Paul Gabrielli

► **To cite this version:**

Mounir Faddaoui, Antoine Folacci, Paul Gabrielli. Surface polaritons of a left-handed curved slab. 2010. hal-00503225

**HAL Id: hal-00503225**

**<https://hal.science/hal-00503225>**

Preprint submitted on 17 Jul 2010

**HAL** is a multi-disciplinary open access archive for the deposit and dissemination of scientific research documents, whether they are published or not. The documents may come from teaching and research institutions in France or abroad, or from public or private research centers.

L'archive ouverte pluridisciplinaire **HAL**, est destinée au dépôt et à la diffusion de documents scientifiques de niveau recherche, publiés ou non, émanant des établissements d'enseignement et de recherche français ou étrangers, des laboratoires publics ou privés.

# Surface polaritons of a left-handed curved slab

Mounir Faddaoui,<sup>1,\*</sup> Antoine Folacci,<sup>1,†</sup> and Paul Gabrielli<sup>2,‡</sup>

<sup>1</sup>*UMR CNRS 6134 SPE, Equipe Physique Théorique,  
Université de Corse, Faculté des Sciences, Boîte Postale 52, 20250 Corte, France*

<sup>2</sup>*UMR CNRS 6134 SPE, Equipe Ondes et Acoustique,  
Université de Corse, Faculté des Sciences, Boîte Postale 52, 20250 Corte, France*

We study the propagation of surface polaritons in a left-handed curved slab, i.e. a curved slab made of a negative-refractive-index material. We consider the effects of the slab curvature on their dispersion relations and attenuations. We show more particularly that surface polaritons with a “left-handed behavior” (i.e. with opposite group and phase velocities) propagate without any attenuation.

PACS numbers: 240.5420, 230.7400, 350.3618, 250.5403

## I. INTRODUCTION

Recently, motivated by theoretical considerations developed a long time ago by Veselago [1] and following insights from Pendry and coworkers [2–4], Shelby, Schultz, Smith and colleagues [5–7] have been able to build, for the first time, by combining arrays of wires and split-ring resonators, an artificial medium for which the electric permittivity, the magnetic permeability and therefore the refractive index are simultaneously negative in the microwave frequency range. They have thus opened a new era for optics because in negative-refractive-index media (also called left-handed materials or double-negative media), electromagnetism presents unusual properties due to various anomalous effects such as reversed Doppler shift, reversed Cerenkov radiation, negative radiation pressure and inverse Snell-Descartes law [1, 8]. Since then, several other groups have successfully fabricated left-handed media and it is now possible to test and to exploit “left-handed electromagnetism” in a large range of frequencies. Of course, the unusual and remarkable properties of negative-refractive-index media could revolutionize optics, optoelectronics and communications and, as a consequence, this recent and rapidly evolving new field of physics has attracted interest of many researchers and many technological applications are already considered including superlenses, band-pass filters, beam guiders, light-emitting devices, cloaking devices ...

In this article, we shall focus our attention on a particular problem of left-handed electromagnetism namely the propagation of surface polaritons in a curved slab made of a negative-refractive-index material and we shall study the effects of curvature on their dispersion relations and attenuations. Surface polaritons (and other guided modes) supported by a left-handed flat slab have been studied extensively in the recent years (see, e.g., [9–18]) due to the central role that they seem to play in the

superlensing phenomenon [11, 19–21] and in the giant Goos-Hänchen effect [22] as well as due to their other potential applications, for example, if we have in mind the development of unconventional photonic integrated circuits and ultra-compact plasmon-based integrated circuits.

In the left-handed flat slab configuration, we can consider that the properties of surface polaritons are now completely known. They have been obtained from rather elementary calculations involving homogeneous and inhomogeneous plane waves. To our knowledge, there exists no description of surface polaritons guided by a left-handed curved slab despite the interest of this problem. Indeed, these surface polaritons are necessary in order to explain the resonant behavior of hollow left-handed nanoparticles [23] or of coaxial cylindrical cables made of negative-index metamaterials [24] and they could be used to transmit efficiently information by using curved waveguides. Mathematically, the description of surface polaritons guided by curved interfaces can be achieved in the framework of complex angular momentum techniques or, in other words, by using the Regge pole machinery [25–28]. In optics, such techniques permit one to naturally shed light on the physics lying behind the transcendental equations involving non-elementary special functions which usually appear in the description of surface waves propagating close to a curved interface. Recently, these techniques have been used in order to describe surface polaritons guided by single interfaces separating a dispersive medium and an ordinary one (see [29–35]). In the present article, we shall apply these techniques in order to analyze the properties of surface polaritons guided in a left-handed cylindrical slab.

Our paper is organized as follows. In Section 2, we briefly recall the theory of surface polaritons guided in a left-handed flat slab embedded in an ordinary dielectric medium. We note that these surface polaritons propagate without any losses and we more particularly emphasize the existence of frequency ranges where they present a “left-handed behavior”, i.e. with opposite group and phase velocities. In Section 3, we extend our analysis to the case of a left-handed cylindrical slab and we consider the effects of its curvature on surface polariton properties.

---

\*Electronic address: faddaoui@univ-corse.fr

†Electronic address: folacci@univ-corse.fr

‡Electronic address: gabrieli@univ-corse.fr

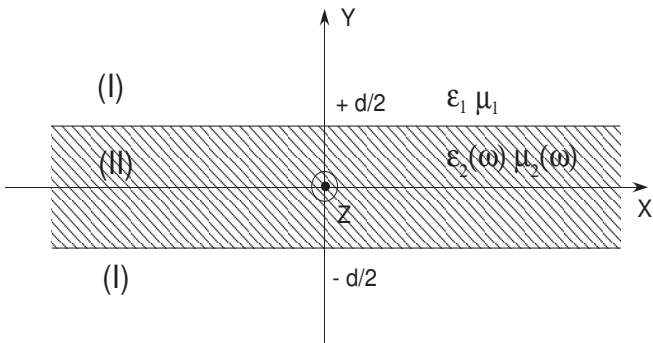


FIG. 1: Geometry of the left-handed slab.

We observe that curvature slightly modifies the dispersion relations of the surface polaritons while, in general, it can lead to important attenuations. However, it is worth pointing out that curvature does not induce any losses for some surface polaritons and, in particular, for those presenting a left-handed behavior. In Section 4, we recall the main results of our work and briefly discuss some possible practical applications.

It should be noted that, in our article, we implicitly assume the time dependence  $\exp(-i\omega t)$  for all the fields.

## II. SURFACE POLARITONS OF A LEFT-HANDED ORDINARY SLAB

### A. General remarks and notations

We consider a symmetric slab of thickness  $d$  made of a negative-refractive-index material (region II) imbedded in a host medium (region I) with electric permittivity  $\epsilon_1 > 0$  and magnetic permeability  $\mu_1 > 0$  both frequency independent (see Fig. 1 for the geometry of the system and the notations). As far as the electric permittivity  $\epsilon_2(\omega)$  and the magnetic permeability  $\mu_2(\omega)$  of the slab are concerned, we assume they are respectively given by

$$\epsilon_2(\omega) = 1 - \frac{\omega_p^2}{\omega^2} \quad (1)$$

and

$$\mu_2(\omega) = 1 - \frac{F\omega^2}{\omega^2 - \omega_0^2} = (1 - F) \left( \frac{\omega^2 - \omega_b^2}{\omega^2 - \omega_0^2} \right) \quad (2)$$

where  $0 < F < 1$  and  $\omega_b = \omega_0/\sqrt{1-F}$ . Of course, the parameters  $\omega_p$ ,  $\omega_0$  and  $F$  depend on the structure of the negative-refractive-index material but we do not attribute any “microscopic” interpretation to them. We only assume that  $\omega_0 < \omega_b < \omega_p$ . We then have  $\epsilon(\omega) < 0$  in the frequency range  $\omega \in ]0, \omega_p[$  and  $\mu(\omega) < 0$  in the frequency range  $\omega \in ]\omega_0, \omega_b[$ . Thus, the electric permittivity, the magnetic permeability and the refractive index are simultaneously negative in the region  $\omega_0 < \omega < \omega_b$ . In that region the metamaterial presents a left-handed

behavior. Furthermore, in order to describe below wave propagation, we also introduce the refractive indices

$$n_1 = \sqrt{\epsilon_1 \mu_1}, \quad (3a)$$

$$n_2(\omega) = \sqrt{\epsilon_2(\omega) \mu_2(\omega)}, \quad (3b)$$

as well as the wave numbers

$$\kappa_1(\omega) = n_1 \left( \frac{\omega}{c} \right), \quad (4a)$$

$$\kappa_2(\omega) = n_2(\omega) \left( \frac{\omega}{c} \right). \quad (4b)$$

We shall study the guided modes propagating along the slab. Here and from now on, we choose to treat our problem in a two-dimensional setting, ignoring the  $z$  coordinate. We shall consider separately the  $H$  and  $E$  polarizations. For the  $H$  polarization, the magnetic field  $\mathbf{H}$  is parallel to the  $z$  axis and, from Maxwell’s equations, it is easy to show that it satisfies the Helmholtz equation

$$\left[ \Delta + n_2^2(\omega) \left( \frac{\omega}{c} \right)^2 \right] H_z^{\text{II}}(\mathbf{x}) = 0 \text{ for } -d/2 < y < d/2, \quad (5a)$$

$$\left[ \Delta + n_1^2 \left( \frac{\omega}{c} \right)^2 \right] H_z^{\text{I}}(\mathbf{x}) = 0 \text{ for } y < -d/2 \text{ and } y > d/2, \quad (5b)$$

where  $\mathbf{x} = (x, y)$ . From the continuity of the tangential components of the electric and magnetic fields at the interface between regions I and II, it can be shown that the  $z$ -component of the magnetic field satisfies, for  $y = \pm d/2$ ,

$$H_z^{\text{I}}(\mathbf{x}) = H_z^{\text{II}}(\mathbf{x}), \quad (6a)$$

$$\frac{1}{\epsilon_1} \frac{\partial H_z^{\text{I}}}{\partial n}(\mathbf{x}) = \frac{1}{\epsilon_2(\omega)} \frac{\partial H_z^{\text{II}}}{\partial n}(\mathbf{x}). \quad (6b)$$

For the  $E$  polarization, the electric field  $\mathbf{E}$  is parallel to the  $z$  axis and, from Maxwell’s equations, we obtain the Helmholtz equation

$$\left[ \Delta + n_2^2(\omega) \left( \frac{\omega}{c} \right)^2 \right] E_z^{\text{II}}(\mathbf{x}) = 0 \text{ for } -d/2 < y < d/2, \quad (7a)$$

$$\left[ \Delta + n_1^2 \left( \frac{\omega}{c} \right)^2 \right] E_z^{\text{I}}(\mathbf{x}) = 0 \text{ for } y < -d/2 \text{ and } y > d/2. \quad (7b)$$

Due to the continuity of the tangential components of the electric and magnetic fields at the interface between regions I and II, the  $z$ -component of the electric field satisfies, for  $y = \pm d/2$ ,

$$E_z^{\text{I}}(\mathbf{x}) = E_z^{\text{II}}(\mathbf{x}), \quad (8a)$$

$$\frac{1}{\mu_1} \frac{\partial E_z^{\text{I}}}{\partial n}(\mathbf{x}) = \frac{1}{\mu_2(\omega)} \frac{\partial E_z^{\text{II}}}{\partial n}(\mathbf{x}). \quad (8b)$$

Finally, it should be noted that the mathematical solutions of the two previous problems can be separated into even (or symmetric) and odd (or antisymmetric) modes due to the symmetry of the slab under the transformation  $y \rightarrow -y$ .

### B. Surface polaritons for the H polarization

For the  $H$  polarization the guided modes propagating in the slab are solutions of the Helmholtz equation (5) of the form

$$\mathbf{H} = \begin{cases} H_1 e^{ikx - \alpha y} \mathbf{e}_z & \text{for } y > \frac{d}{2}, \\ H_2 e^{ikx} f_{\pm}(\beta y) \mathbf{e}_z & \text{for } -\frac{d}{2} < y < \frac{d}{2}, \\ \pm H_1 e^{ikx + \alpha y} \mathbf{e}_z & \text{for } y < -\frac{d}{2}, \end{cases} \quad (9)$$

with  $f_+(\beta y) = \cosh(\beta y)$  and  $f_-(\beta y) = \sinh(\beta y)$ . In Eq. (9) the + and - signs are respectively associated with even and odd modes. Here  $k$  describes the propagation of the magnetic field along the  $x$  axis, while  $\alpha$  and  $\beta$  are functions permitting us to describe its decay near the interfaces. By inserting Eq. (9) into Eqs. (5) and (6), we obtain from one hand

$$\alpha^2(\omega, k) = k^2 - \kappa_1^2(\omega), \quad (10)$$

$$\beta^2(\omega, k) = \kappa_2^2(\omega) - k^2, \quad (11)$$

and from the other hand

$$\frac{\alpha(\omega, k)}{\beta(\omega, k)} = -\frac{\varepsilon_1}{\varepsilon_2(\omega)} \tanh\left[\frac{\beta(\omega, k)d}{2}\right], \quad (12)$$

$$H_2 = H_1 \frac{\exp\left[-\frac{\alpha(\omega, k)d}{2}\right]}{\cosh\left[\frac{\beta(\omega, k)d}{2}\right]}, \quad (13)$$

for the even solutions, and

$$\frac{\alpha(\omega, k)}{\beta(\omega, k)} = -\frac{\varepsilon_1}{\varepsilon_2(\omega)} \coth\left[\frac{\beta(\omega, k)d}{2}\right], \quad (14)$$

$$H_2 = H_1 \frac{\exp\left[-\frac{\alpha(\omega, k)d}{2}\right]}{\sinh\left[\frac{\beta(\omega, k)d}{2}\right]}, \quad (15)$$

for the odd solutions. Equations (12) and (14) provide implicitly, for the  $H$  polarization, the dispersion relations  $k = k(\omega)$  or  $\omega = \omega(k)$  for the guided modes propagating in the slab. From now on, we shall only consider the guided surface modes. We then require the following conditions

$$\alpha^2(\omega, k) > 0 \text{ and } \beta^2(\omega, k) < 0,$$

which imply

$$k^2 > \kappa_1^2(\omega), \quad (16a)$$

$$k^2 > \kappa_2^2(\omega), \quad (16b)$$

for the existence conditions of the surface polaritons.

### C. Surface polaritons for the E polarization

For the  $E$  polarization the guided modes propagating in the slab are solutions of the Helmholtz equation (7) of the form

$$\mathbf{E} = \begin{cases} E_1 e^{ikx - \alpha y} \mathbf{e}_z & \text{for } y > \frac{d}{2}, \\ E_2 e^{ikx} f_{\pm}(\beta y) \mathbf{e}_z & \text{for } -\frac{d}{2} < y < \frac{d}{2}, \\ \pm E_1 e^{ikx + \alpha y} \mathbf{e}_z & \text{for } y < -\frac{d}{2}, \end{cases} \quad (17)$$

with  $f_+(\beta y) = \cosh(\beta y)$  and  $f_-(\beta y) = \sinh(\beta y)$ . Here  $k$ ,  $\alpha$  and  $\beta$  as well as the + and - signs keep their previous interpretations. Substituting Eq. (17) into Eq. (7) provides again the relations (10) and (11). Moreover, by inserting (17) into (8), we obtain

$$\frac{\alpha(\omega, k)}{\beta(\omega, k)} = -\frac{\mu_1}{\mu_2(\omega)} \tanh\left[\frac{\beta(\omega, k)d}{2}\right], \quad (18)$$

$$E_2 = E_1 \frac{\exp\left[-\frac{\alpha(\omega, k)d}{2}\right]}{\cosh\left[\frac{\beta(\omega, k)d}{2}\right]}, \quad (19)$$

for the even solutions, and

$$\frac{\alpha(\omega, k)}{\beta(\omega, k)} = -\frac{\mu_1}{\mu_2(\omega)} \coth\left[\frac{\beta(\omega, k)d}{2}\right], \quad (20)$$

$$E_2 = E_1 \frac{\exp\left[-\frac{\alpha(\omega, k)d}{2}\right]}{\sinh\left[\frac{\beta(\omega, k)d}{2}\right]}, \quad (21)$$

for the odd solutions. Equations (18) and (20) provide implicitly, for the  $E$  polarization, the dispersion relations  $k = k(\omega)$  or  $\omega = \omega(k)$  for the guided modes propagating in the slab and we still have the existence conditions (16) for the surface polaritons.

### D. Numerical aspects

In Fig. 2 we display the surface polariton dispersion relations for the slab embedded in vacuum ( $\varepsilon_1 = 1$  and  $\mu_1 = 1$ ). They are plotted in the form  $k_r = k_r(\omega_r)$  where  $k_r$  and  $\omega_r$  are the reduced parameters defined by

$$k_r = \frac{kd}{c}, \quad (22a)$$

$$\omega_r = \frac{\omega d}{c}. \quad (22b)$$

As far as the characteristics of the left-handed material are concerned, we work with  $F = 0.4$  and with the reduced frequencies  $\omega_{r0} = \omega_0 d/c = 0.552$ ,  $\omega_{rb} = \omega_b d/c \approx 0.7127$  and  $\omega_{rp} = \omega_p d/c = 1.104$ . Even though we restrict ourselves to that particular configuration, the results we obtain numerically are in fact very general and

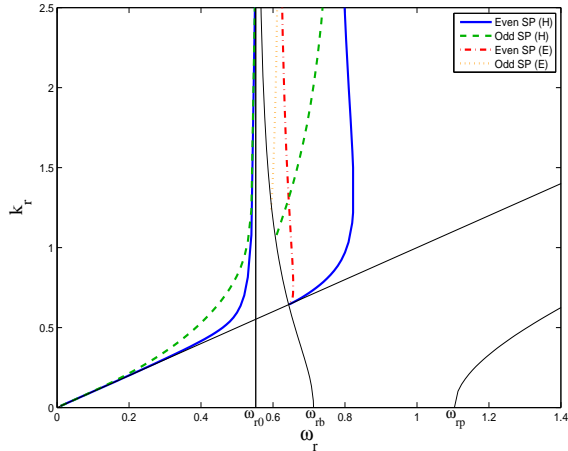


FIG. 2: Dispersion relations of the surface polaritons for a left-handed flat slab embedded in vacuum ( $\varepsilon_1 = 1$ ,  $\mu_1 = 1$ ). The tiny curves delimit the regions in which surface polaritons can exist (cf. Eqs. (16)).

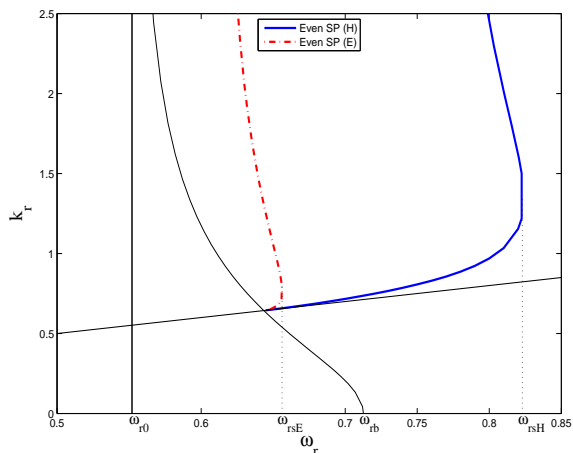


FIG. 3: Zoom in on dispersion relations of the even surface polaritons with “left-handed behavior”. The left-handed flat slab is embedded in vacuum ( $\varepsilon_1 = 1$ ,  $\mu_1 = 1$ ).

they permit us to correctly illustrate the theory. Similarly, the global aspects of the dispersion curves are rather independent of the value of  $\varepsilon_1$ .

Our results are in agreement with those already obtained in the literature by several authors (see e.g. Ref. [9]). So, we shall not lengthily analyze them. However we would like to emphasize the slope inversion (as well as its consequences) which occurs for the two branches corresponding to the even surface polaritons in the frequency range  $\omega_{r0} < \omega_r < \omega_{rpb}$ . Indeed, let us denote by  $\omega_{rsH}$  and  $\omega_{rsE}$  the slope inversion frequencies of the even surface polaritons for the  $H$  and  $E$  polarizations (see Fig. 3). In the  $H$  polarization case, for  $\omega_r$  below but near  $\omega_{rsH}$  there exist two values for the reduced propagation

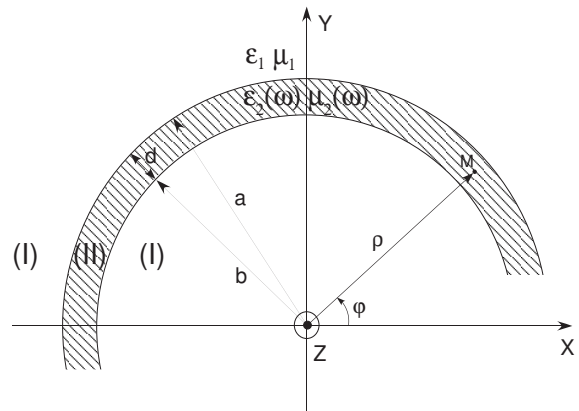


FIG. 4: Geometry of the left-handed curved slab.

constant  $k_r$  corresponding to two distinct behavior for the surface polaritons:

- (i) for the lower  $k_r$  value, the slope is positive and, as a consequence, the group and phase velocities are both positive and the surface polariton presents an ordinary behavior,
- (ii) for the higher  $k_r$  value, the slope is negative and, as a consequence, the group and phase velocities are opposite and the surface polariton presents a left-handed behavior.

Such a result will have a crucial importance for surface polaritons propagating in a curved slab. In the  $E$  polarization case, similar considerations apply with  $\omega_{rsE}$  replacing  $\omega_{rsH}$ .

### III. SURFACE POLARITONS OF A LEFT-HANDED CURVED SLAB

#### A. General remarks and notations

We assume that the previous slab of thickness  $d = a - b$  has been bent and occupies the region corresponding to the range  $b < \rho < a$  in the usual cylindrical coordinate system  $(\rho, \varphi, z)$  (see Fig. 4).

We shall study the guided modes propagating along the slab by treating again our problem in a two-dimensional setting (ignoring the  $z$  coordinate) and considering separately the  $H$  and  $E$  polarizations. For the  $H$  polarization, the magnetic field  $\mathbf{H}$  is parallel to the  $z$  axis and, from Maxwell's equations, it is easy to show that it satisfies

the Helmholtz equation

$$\left[ \Delta + n_2^2(\omega) \left( \frac{\omega}{c} \right)^2 \right] H_z^{\text{II}}(\mathbf{x}) = 0 \quad \text{for } b < \rho < a, \quad (23a)$$

$$\left[ \Delta + n_1^2 \left( \frac{\omega}{c} \right)^2 \right] H_z^{\text{I}}(\mathbf{x}) = 0 \quad \text{for } 0 < \rho < b \text{ and } \rho > a, \quad (23b)$$

where  $\mathbf{x} = (\rho, \varphi)$ . From the continuity of the tangential components of the electric and magnetic fields at the interface between regions I and II, we can show that the relations (6) remain valid for  $\rho = a$  and  $\rho = b$ . For the  $E$  polarization, the electric field  $\mathbf{E}$  is parallel to the  $z$  axis and, from Maxwell's equations, we obtain the Helmholtz equation

$$\left[ \Delta + n_2^2(\omega) \left( \frac{\omega}{c} \right)^2 \right] E_z^{\text{II}}(\mathbf{x}) = 0 \quad \text{for } b < \rho < a, \quad (24a)$$

$$\left[ \Delta + n_1^2 \left( \frac{\omega}{c} \right)^2 \right] E_z^{\text{I}}(\mathbf{x}) = 0 \quad \text{for } 0 < \rho < b \text{ and } \rho > a. \quad (24b)$$

Due to the continuity of the tangential components of the electric and magnetic fields at the interface between regions I and II, the  $z$ -component of the electric field again satisfies the relations (8) for  $\rho = a$  and  $\rho = b$ . Finally, it should be noted that the mathematical solutions of the

two previous problems cannot be naturally separated into even (or symmetric) and odd (or antisymmetric) modes due to the symmetry breaking induced by the curvature of the slab.

## B. Surface polaritons for the H polarization

For the  $H$  polarization the guided modes propagating in the slab are solutions of the Helmholtz equation (23) which can be expressed in terms of Bessel functions [36] on the form  $\mathbf{H} = H_z \mathbf{e}_z$  with

$$H_z(\rho, \varphi) = \begin{cases} A_1 H_\lambda^{(1)}[\kappa_1(\omega)\rho] e^{i\lambda\varphi} & \text{for } \rho > a, \\ \left( A_2 J_\lambda[\kappa_2(\omega)\rho] + B_2 H_\lambda^{(1)}[\kappa_2(\omega)\rho] \right) e^{i\lambda\varphi} & \text{for } b < \rho < a, \\ A_3 J_\lambda[\kappa_1(\omega)\rho] e^{i\lambda\varphi} & \text{for } 0 < \rho < b. \end{cases} \quad (25)$$

Here  $\lambda$  is an azimuthal complex constant describing the propagation along the curved slab while  $\kappa_1(\omega)$  and  $\kappa_2(\omega)$  are still defined by Eqs. (4). Substituting (25) into (6) provides a system of four equations with four unknowns that can be expressed in the matrix form

$$M^H(\lambda, \omega) C^H = 0 \quad (26)$$

with

$$M^H(\lambda, \omega) = \begin{pmatrix} H_\lambda^{(1)}[\kappa_1(\omega)a] & -J_\lambda[\kappa_2(\omega)a] & -H_\lambda^{(1)}[\kappa_2(\omega)a] & 0 \\ \sqrt{\frac{\mu_1}{\varepsilon_1}} H_\lambda^{(1)'}[\kappa_1(\omega)a] & -\sqrt{\frac{\mu_2(\omega)}{\varepsilon_2(\omega)}} J_\lambda'[\kappa_2(\omega)a] & -\sqrt{\frac{\mu_2(\omega)}{\varepsilon_2(\omega)}} H_\lambda^{(1)'}[\kappa_2(\omega)a] & 0 \\ 0 & -\sqrt{\frac{\mu_2(\omega)}{\varepsilon_2(\omega)}} J_\lambda'[\kappa_2(\omega)b] & -\sqrt{\frac{\mu_2(\omega)}{\varepsilon_2(\omega)}} H_\lambda^{(1)'}[\kappa_2(\omega)b] & \sqrt{\frac{\mu_1}{\varepsilon_1}} J_\lambda'[\kappa_1(\omega)b] \\ 0 & -J_\lambda[\kappa_2(\omega)b] & -H_\lambda^{(1)}[\kappa_2(\omega)b] & J_\lambda[\kappa_1(\omega)b] \end{pmatrix} \quad (27)$$

and

$$C^H = \begin{pmatrix} A_1 \\ A_2 \\ B_2 \\ A_3 \end{pmatrix}. \quad (28)$$

The system (26) admits non trivial solutions  $C^H$  only if

$$\det M^H(\lambda, \omega) = 0. \quad (29)$$

The complex solutions  $\lambda$  of Eq. (29) are the so-called Regge poles and they can be interpreted as complex angular momenta [25–28]. The relations  $\lambda = \lambda(\omega)$  obtained from (29) provide the dispersion relation as well as the attenuation of all the guided modes propagating in the slab. Among all these modes, there exist guided modes corresponding to those already present in the ordinary

slab, as well as an infinity of new modes due to the slab curvature (whispering gallery modes). Of course, we shall focus our attention only to the guided modes associated with the surface polaritons described in Section 2.

## C. Surface polaritons for the E polarization

For the  $E$  polarization the guided modes propagating in the slab are solutions of the Helmholtz equation (24) of the form  $\mathbf{E} = E_z \mathbf{e}_z$  with

$$E_z(\rho, \varphi) = \begin{cases} A_1 H_\lambda^{(1)}[\kappa_1(\omega)\rho] e^{i\lambda\varphi} & \text{for } \rho > a, \\ \left( A_2 J_\lambda[\kappa_2(\omega)\rho] + B_2 H_\lambda^{(1)}[\kappa_2(\omega)\rho] \right) e^{i\lambda\varphi} & \text{for } b < \rho < a, \\ A_3 J_\lambda[\kappa_1(\omega)\rho] e^{i\lambda\varphi} & \text{for } 0 < \rho < b. \end{cases} \quad (30)$$

Substituting (30) into (8) provides a system of four equations with four unknowns that can be expressed in the matrix form

$$M^E(\lambda, \omega) C^E = 0 \quad (31)$$

with

$$M^E(\lambda, \omega) = \begin{pmatrix} H_\lambda^{(1)}[\kappa_1(\omega) a] & -J_\lambda[\kappa_2(\omega) a] & -H_\lambda^{(1)}[\kappa_2(\omega) a] & 0 \\ \sqrt{\frac{\varepsilon_1}{\mu_1}} H_\lambda^{(1)'}[\kappa_1(\omega) a] & -\sqrt{\frac{\varepsilon_2(\omega)}{\mu_2(\omega)}} J_\lambda'[\kappa_2(\omega) a] & -\sqrt{\frac{\varepsilon_2(\omega)}{\mu_2(\omega)}} H_\lambda^{(1)'}[\kappa_2(\omega) a] & 0 \\ 0 & -\sqrt{\frac{\varepsilon_2(\omega)}{\mu_2(\omega)}} J_\lambda'[\kappa_2(\omega) b] & -\sqrt{\frac{\varepsilon_2(\omega)}{\mu_2(\omega)}} H_\lambda^{(1)'}[\kappa_2(\omega) b] & \sqrt{\frac{\varepsilon_1}{\mu_1}} J_\lambda'[\kappa_1(\omega) b] \\ 0 & -J_\lambda[\kappa_2(\omega) b] & -H_\lambda^{(1)}[\kappa_2(\omega) b] & J_\lambda[\kappa_1(\omega) b] \end{pmatrix} \quad (32)$$

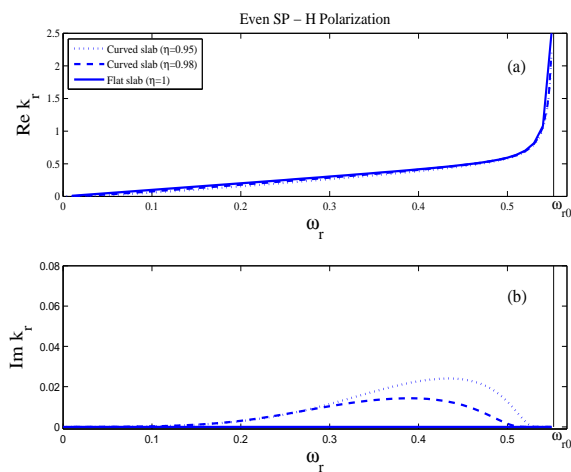


FIG. 5: Dispersion relations (a) and attenuations (b) of surface polaritons guided in left-handed flat and curved slabs embedded in vacuum ( $\varepsilon_1 = 1$ ,  $\mu_1 = 1$ ): role of the slab curvature. Even surface polariton,  $H$  polarization, frequency range  $0 < \omega_r < \omega_{r0}$ .

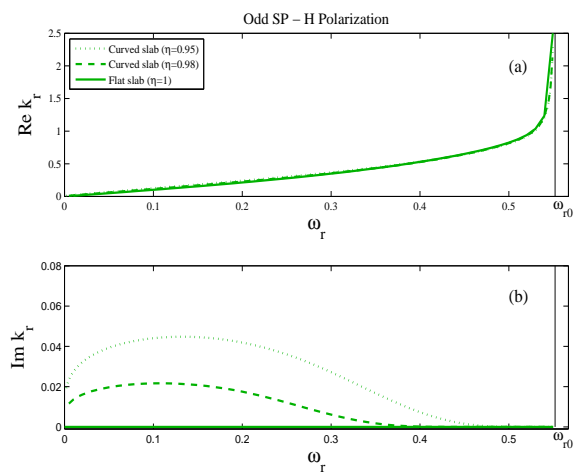


FIG. 6: Dispersion relations (a) and attenuations (b) of surface polaritons guided in left-handed flat and curved slabs embedded in vacuum ( $\varepsilon_1 = 1$ ,  $\mu_1 = 1$ ): role of the slab curvature. Odd surface polariton,  $H$  polarization, frequency range  $0 < \omega_r < \omega_{r0}$ .

and

$$C^E = \begin{pmatrix} A_1 \\ A_2 \\ B_2 \\ A_3 \end{pmatrix}. \quad (33)$$

The system (31) admits non trivial solutions  $C^E$  only if

$$\det M^E(\lambda, \omega) = 0 \quad (34)$$

which provides the dispersion relation and the attenuation of all the guided modes propagating in the slab. Similarly, we shall focus our attention only to the guided modes associated with the surface polaritons described in Section 2.

#### D. Numerical aspects

We shall restrict our numerical study to cylindrical slabs of weak curvature. In other words, we shall assume that  $d \ll a$  and  $d \ll b$  and therefore that  $\eta = b/a \approx 1$ . This hypothesis permits us to consider that surface polaritons propagate very close to  $\rho = a$  and thus the arc length they cover is given by  $\mathcal{L} = a\varphi$ . As a consequence, the complex wave number  $k$  describing propagation along the curved slab is linked to the complex angular momentum  $\lambda$  by  $k = \lambda/a$  [in Eqs. (25) and (30), we can write  $\exp(i\lambda\varphi) = \exp(ik\mathcal{L})$ ] and therefore  $\text{Re } k = \text{Re } \lambda/a$  and  $\text{Im } k = \text{Im } \lambda/a$  provide respectively the dispersion relation and the attenuation of surface polaritons.

In Figs. 5-12 we display the dispersion relations and the attenuations of the surface polaritons guided in the left-handed cylindrical slab embedded in vacuum ( $\varepsilon_1 = 1$

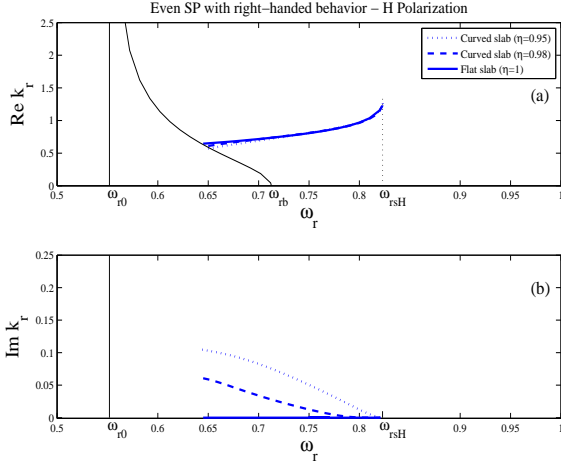


FIG. 7: Dispersion relations (a) and attenuations (b) of surface polaritons guided in left-handed flat and curved slabs embedded in vacuum ( $\varepsilon_1 = 1$ ,  $\mu_1 = 1$ ): role of the slab curvature. Even surface polariton with right-handed behavior,  $H$  polarization, frequency range  $\omega_r > \omega_{r0}$ .

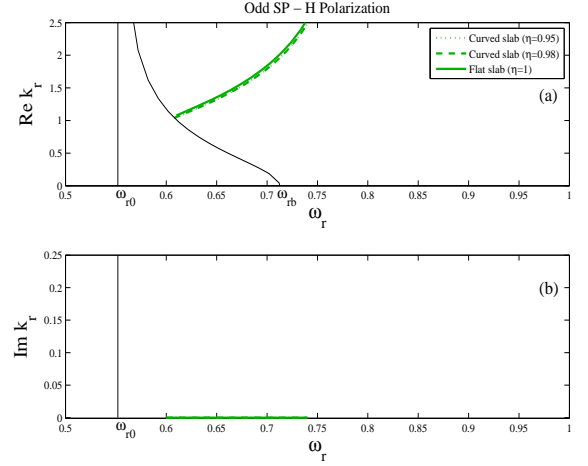


FIG. 9: Dispersion relations (a) and attenuations (b) of surface polaritons guided in left-handed flat and curved slabs embedded in vacuum ( $\varepsilon_1 = 1$ ,  $\mu_1 = 1$ ): role of the slab curvature. Odd surface polariton,  $H$  polarization, frequency range  $\omega_r > \omega_{r0}$ .

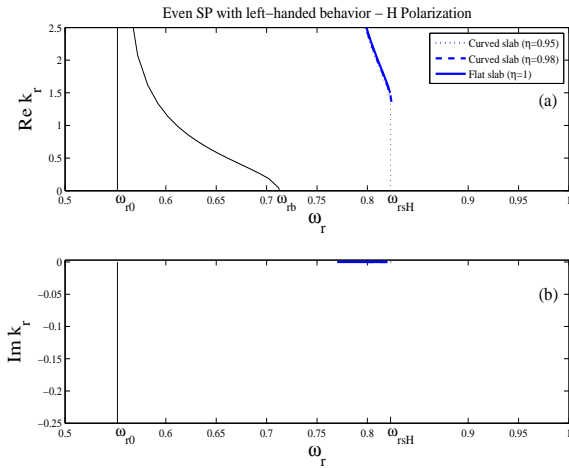


FIG. 8: Dispersion relations (a) and attenuations (b) of surface polaritons guided in left-handed flat and curved slabs embedded in vacuum ( $\varepsilon_1 = 1$ ,  $\mu_1 = 1$ ): role of the slab curvature. Even surface polariton with left-handed behavior,  $H$  polarization, frequency range  $\omega_r > \omega_{r0}$ .

and  $\mu_1 = 1$ ). Even though we have restricted ourselves to that configuration, the results we obtained numerically are in fact very general and they permit us to correctly illustrate the theory. In particular, the global aspects of the dispersion and attenuation curves are rather independent of the value of  $\varepsilon_1$ . These curves are plotted in the form  $\text{Re } k_r = \text{Re } k_r(\omega_r)$  and  $\text{Im } k_r = \text{Im } k_r(\omega_r)$  where  $k_r$  is the reduced wave number

$$k_r = \frac{\lambda d}{ac} \quad (35)$$

while  $\omega_r$  is the reduced frequency already defined in Eq.

(22b). The characteristics of the left-handed material are those previously given in Section 2.D. Here, it is important to note that (i) we use the same definition of the reduced frequency  $\omega_r$  for both the flat and the curved slab and (ii) the case of the flat slab examined in the previous section can be formally recovered by taking the limit  $\eta \rightarrow 1$  and keeping  $d = (a - b) = \text{const}$ . These considerations permit us to compare on same plots the properties of the surface polaritons guided in flat ( $\eta = 1$ ) and curved ( $\eta = 0.95$  and  $\eta = 0.98$ ) slabs. It should be also noted that we have kept the terminology “even” and “odd” in spite of the symmetry breaking induced by the curvature of the slab.

In Figs. 5-12 we can see that the surface polariton dispersion relations change only very little with the slab curvature. In Figs. 5, 6, 7, 10 we can observe that curvature induces attenuation of the considered surface polaritons. This is in accordance with the usual behavior of surface polaritons guided by curved interfaces and it can be interpreted in terms of energy radiated away from the interfaces. Such a behavior does not occur for the surface polaritons described in Figs. 8, 9, 11, 12 where no attenuation is observed. This is of course very surprising and constitutes the main result of our study. This is observed in the frequency range  $\omega_r > \omega_{r0}$  for the “odd” surface polaritons and for the “even” surface polaritons with left-handed behavior.

#### IV. CONCLUSION

In this article, we have described the surface polaritons guided in a left-handed cylindrical slab. We have shown that the slab curvature slightly modifies the sur-



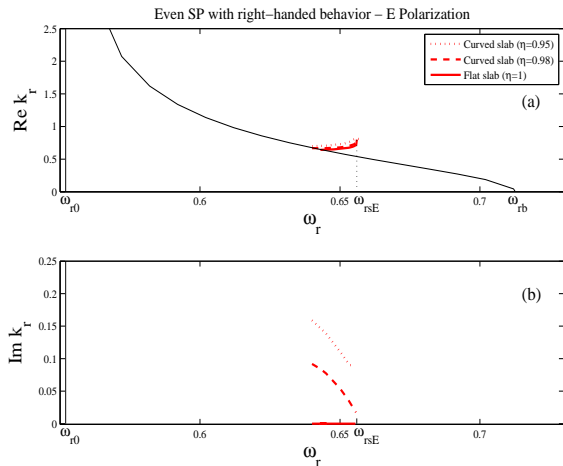


FIG. 10: Dispersion relations (a) and attenuations (b) of surface polaritons guided in left-handed flat and curved slabs embedded in vacuum ( $\epsilon_1 = 1$ ,  $\mu_1 = 1$ ): role of the slab curvature. Even surface polariton with right-handed behavior,  $E$  polarization, frequency range  $\omega_r > \omega_{r0}$ .

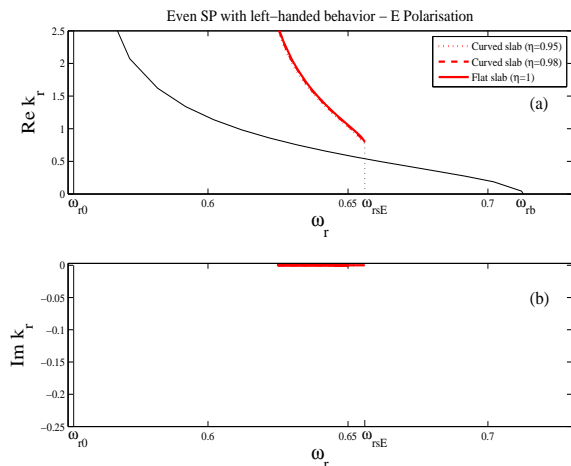


FIG. 11: Dispersion relations (a) and attenuations (b) of surface polaritons guided in left-handed flat and curved slabs embedded in vacuum ( $\epsilon_1 = 1$ ,  $\mu_1 = 1$ ): role of the slab curvature. Even surface polariton with left-handed behavior,  $E$  polarization, frequency range  $\omega_r > \omega_{r0}$ .

face polariton dispersion relations. It is well known that, in general, curvature induces attenuation of surface polaritons due to energy radiated away from the interfaces. However, it is worth pointing out that for the left-handed cylindrical slab, under certain conditions, surface polaritons

can propagate without loss. This is true, in particular, for the surface polaritons presenting a left-handed behavior.

Surface polaritons propagating without attenuation are particularly useful with in mind practical applications in the field of optical communications as well as the development of photonic integrated circuits and ultra-compact

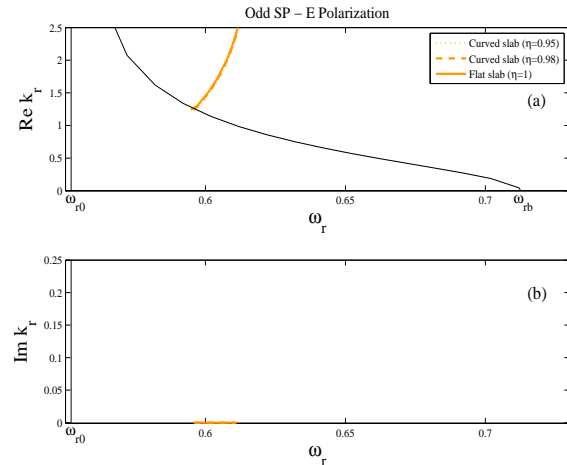


FIG. 12: Dispersion relations (a) and attenuations (b) of surface polaritons guided in left-handed flat and curved slabs embedded in vacuum ( $\epsilon_1 = 1$ ,  $\mu_1 = 1$ ): role of the slab curvature. Odd surface polariton,  $E$  polarization, frequency range  $\omega_r > \omega_{r0}$ .

plasmon-based integrated circuits. It is therefore very interesting to know that it is possible to transmit information without loss by using left-handed curved waveguides and that this can be achieved by using surface polaritons with unusual properties.

Finally, it should be noted that, in this article, we have restricted to surface polaritons our study of the modes guided in a left-handed curved slab. It is important to recall that such a waveguide is in fact a very rich system: indeed, in addition to the surface polaritons considered here, there also exists an infinite family of oscillating guided modes already present on the left-handed flat slab as well as an infinity of new guided modes of whispering-gallery-type which have no analogs in the flat slab case. They could also play an important role in the context of nanoparticle physics (in order to fully understand the resonant properties of hollow spheres made of a negative-refractive-index material) or in the context of optical transmission of information.

[1] V. G. Veselago, "The electrodynamics of substances with simultaneously negative values of  $\epsilon$  and  $\mu$ ," *Sov. Phys. Usp.* **10**, 509-514 (1968)

[2] J. B. Pendry, A. J. Holden, W. J. Stewart and I. Youngs, "Extremely low frequency plasmons in metallic mesostructures," *Phys. Rev. Lett.* **76**, 4773-4776 (1996)

- [3] J. B. Pendry, A. J. Holden, D. J. Robbins and W. J. Stewart, "Low frequency plasmons in thin wire structures," *J. Phys.: Condens. Matter* **10**, 4785-4809 (1998)
- [4] J. B. Pendry, A. J. Holden, D. J. Robbins and W. J. Stewart, "Magnetism from conductors and enhanced nonlinear phenomena," *IEEE Trans. Microwave Theory Tech.* **47**, 2075-2084 (1999)
- [5] D. R. Smith, W. J. Padilla, D. C. Vier, S. C. Nemat-Nasser and S. Schultz, "Composite medium with simultaneously negative permeability and permittivity," *Phys. Rev. Lett.* **84**, 4184-4187 (2000)
- [6] R. A. Shelby, D. R. Smith, S. C. Nemat-Nasser and S. Schultz, "Microwave transmission through a two-dimensional, isotropic, left-handed metamaterial," *Appl. Phys. Lett.* **78**, 489-491 (2001)
- [7] R. A. Shelby, D. R. Smith and S. Schultz, "Experimental verification of a negative index of refraction," *Science* **292**, 77-79 (2001)
- [8] J. B. Pendry and D. R. Smith, "Reversing light with negative refraction," *Phys. Today* **57**, 37-43 (2004)
- [9] R. Ruppin, "Surface polaritons of a left-handed material slab", *J. Phys. : Condens. Matter* **13**, 1811-1819 (2001)
- [10] I. V. Shadrivov, A. A. Sukhorukov and Y. S. Kivshar, "Guided modes in negative-refractive-index waveguides," *Phys. Rev. E* **67**, 057602 (2003)
- [11] X. S. Rao and C. K. Ong, "Amplification of evanescent waves in a lossy left-handed material slab," *Phys. Rev. B* **68**, 113103 (2003)
- [12] K. Park, B. J. Lee, C. Fu, and Z. M. Zhang, "Study of the surface and bulk polaritons with a negative index metamaterial," *J. Opt. Soc. Am. B* **22**, 1016-1023 (2005)
- [13] I. V. Shadrivov, R. W. Ziolkowski, A. A. Zharov and Y. S. Kivshar, "Excitation of guided waves in layered structures with negative refraction," *Opt. Express* **13**, 481-492 (2005)
- [14] Y. He, Z. Cao and Q. Shen, "Guided optical modes in asymmetric left-handed waveguides," *Opt. Commun.* **245**, 125-135 (2005)
- [15] I. V. Shadrivov, A. A. Zharov and Y. S. Kivshar, "Second-harmonic generation in nonlinear left-handed metamaterials," *J. Opt. Soc. Am. B* **23**, 529-534 (2006)
- [16] S. A. Darmanyan, A. Kobayakov and D. Q. Chowdhury, "Nonlinear guided waves in a negative-index slab waveguide," *Phys. Lett. A* **363**, 159-163 (2007)
- [17] A. Moreau and D. Felbacq, "Leaky modes of left-handed slab," *J. Europ. Opt. Soc.* **3**, 08032 (2008)
- [18] Z. H. Wang and S. P. Li, "Quasi-optics of the surface guided modes in a left-handed material slab waveguide," *J. Opt. Soc. Am. B* **25**, 903-908 (2008)
- [19] J. B. Pendry, "Negative refraction makes a perfect lens," *Phys. Rev. Lett.* **85**, 3966-3969 (2000)
- [20] M. W. Feise, P. J. Bevelacqua and J. B. Schneider, "Effects of Surface Waves on the Behavior of Perfect Lenses," *Phys. Rev. B* **66**, 035113 (2002)
- [21] F. D. M. Haldane, "Electromagnetic surface modes at interfaces with negative refractive index make a not-quite-perfect lens," arXiv:cond-mat/0206420 (2002)
- [22] I. V. Shadrivov, A. A. Zharov and Y. S. Kivshar, "Giant Goos-Hanchen effect at the reflection from left-handed metamaterials," *Appl. Phys. Lett.* **83**, 2713-2715 (2003)
- [23] R. Ruppin, "Surface modes and extinction properties of a doubly dispersive spherical shell," *Phys. Lett. A* **337**, 135-140 (2005)
- [24] M. S. Kushwaha and B. Djafari-Rouhani, "Theory of confined plasmonic waves in coaxial cylindrical cables fabricated of metamaterials," *J. Opt. Soc. Am. B* **27**, 148-167 (2010)
- [25] G. N. Watson, "The Diffraction of electric waves by the earth," *Proc. Roy. Soc. London A* **95**, 83-99 (1918)
- [26] A. Sommerfeld, *Partial Differential Equations of Physics* (Academic Press, New York, 1949)
- [27] H. M. Nussenzweig, *Diffraction Effects in Semiclassical Scattering* (Cambridge University Press, Cambridge, 1992)
- [28] W. T. Grandy, Jr, *Scattering of Waves from Large Spheres* (Cambridge University Press, Cambridge, 2000)
- [29] M. V. Berry, "Attenuation and focusing of electromagnetic surface waves rounding gentle bends," *J. Phys. A: Math. Gen.* **8**, 1952-1971 (1975).
- [30] S. Ancey, Y. Décanini, A. Folacci and P. Gabrielli, "Surface polaritons on metallic and semiconducting cylinders: A complex angular momentum analysis," *Phys. Rev. B* **70**, 245406 (2004)
- [31] S. Ancey, Y. Décanini, A. Folacci and P. Gabrielli, "Surface polaritons on left-handed cylinders: A complex angular momentum analysis," *Phys. Rev. B* **72**, 085458 (2005)
- [32] S. Ancey, Y. Décanini, A. Folacci and P. Gabrielli, "Surface polaritons on left-handed spheres," *Phys. Rev. B* **76**, 195413 (2007)
- [33] S. Ancey, Y. Décanini, A. Folacci and P. Gabrielli, "Surface plasmon polaritons and surface phonon polaritons on metallic and semiconducting spheres: Exact and semiclassical descriptions," *J. Opt. Soc. Am. B* **26**, 1176 (2009)
- [34] K. Hasegawa, J. U. Nockel and M. Deutsch, "Surface plasmon polariton propagation around bends at a metal-dielectric interface," *Appl. Phys. Lett.* **84**, 1835-1837 (2004)
- [35] K. Hasegawa, J. U. Nockel and M. Deutsch, "Curvature-induced radiation of surface plasmon polaritons propagating around bends," *Phys. Rev. A* **75**, 063816 (2007)
- [36] M. Abramowitz and I. A. Stegun, *Handbook of Mathematical Functions* (Dover, New-York, 1965)